Effect of Shape and Orientation of Carbon Steel Fiber on the Modulus of Epoxy-Based Composite

M. S. Ghoraishi,[1] A. Zadhoush,[1] A. A. GharehAghaji[2]

[1]*Department of Textile Engineering, Isfahan University of Technology, Isfahan, 84156-83111, Iran*
[2]*Department of Textile Engineering, Amirkabir University of Technology, Tehran, 15875-4413, Iran*

Received 10 April 2010; accepted 20 October 2010
DOI 10.1002/app.33591
Published online 22 February 2011 in Wiley Online Library (wileyonlinelibrary.com).

ABSTRACT: In this research work, the effect of parameters such as orientation, length, and shape of fibers were investigated. Flat and waved carbon steel fibers with 15 mm length were used with different orientations. The effect of orientation and shape of fibers on composite modulus was investigated. Fiber-reinforced epoxy resin with 30 mm waved and endhooked fibers were also investigated. The theoretical results obtained using Halpin-Tsai model are in good agreement with the experimental results for all the shapes and orientations. Because of the mechanical interlock, the shaped fibers can bridge matrix cracks effectively and improve composite's modulus. Improvement of modulus using shaped fibers for certain orientations has been achieved. The results obtained are useful in the application of texturising on the synthetic fibers in polymeric materials and provide flexibility in design of any demanded shape through improving modulus at different angles. © 2011 Wiley Periodicals, Inc. J Appl Polym Sci 121: 469–474, 2011

Key words: composites; modulus; shaped ductile fiber; modeling; thermosetting resin

INTRODUCTION

Short fiber composites are attractive structural material because of their advantages over continues fiber composites. These advantages include low-cost manufacturing methods, ease of fabrication, manufacturing complex shaped structure potential, great versatility, and flexibility of properties based on controlling the flow of material.[1–3]

According to many reported research works, fracture toughness of a brittle matrix composite could be improved by use of short shaped ductile fiber as reinforcement.

In case of incorporating aligned fiber in a matrix with the fiber axis parallel to the loading direction reinforcement can be more significant.[3–5] Also, waved fiber can influence the mechanical properties of textile composite castings.[6] As a result of interfacial debonding and discontinuities at fiber ends, short-fiber polymer composites usually have low strength and toughness in comparison with continuous fiber composites.[7] For short fiber composite, load transfer between the fibers and the matrix can be improved by optimization of the fiber shape and a strong interface. Therefore, overall mechanical performance will be improved. Interface plays a significant role in changing the effective length that carried load in short fiber composite. This effective length can be improved through strong interface and lead to the reduction of ineffective length at both ends of the fiber.[8,9]

Appropriate anchoring of fibers into the matrix can influence toughness flexural strength and modulus. This can be done either by accomplishing a gross physical shape change to create an anchor or by mechanical or chemical changes to the surface to create small anchors to improve pullout work.[10–13] Excellent crack bridging and load transfer mechanism can be achieved if fiber is anchored into the matrix even with a weak interface. Wetherhold and Bös showed that ductile metal short fibers with flattened ends could greatly enhance the fracture resistance of epoxy-based composites.[1]

The mechanism of strength and toughness increase in composite material resulting from the addition of fibers is somehow more complicated. Generally, fibers can bridge the fracture surface, providing a reduction in the net stress intensity factor due to increase in energy dissipation through bridging, often with fiber pullout, fiber fracture or plasticity.[12] Effective load transfer through the fiber/matrix interface has a significant effect on the performance of the composite. Fiber geometries can greatly influence the fiber/matrix load transfer mechanism.[2,7,8,10,14–16]

Theoretical and experimental technique for prediction of the overall effective properties of composite has been the subject of comprehensive studies.[17] Halpin-Tsai model is one of the numerous

Correspondence to: A. Zadhoush (zadhoush@cc.iut.ac.ir).

TABLE I
Material Properties

Materials	Fiber	Matrix
Properties		
Modulus (GPa)	135.80	2.05
Poisson's ratio	0.28	0.30
Volume fraction	3%	97%
Weight fraction	16%	84%

micromechanics-based models for predicting properties of composites for aligned short-fiber composites. This model was derived from the self-consistent models of Hermans and Hill and primarily developed for continuous fiber composites. Because of the fact that the Halpin-Tsai equations can be expressed in a short and easily usable form, as shown by eqs. (1)–(3) these equations have found an extensive usage. The rule of mixtures is also applied to calculate the longitudinal Poisson's ratio υ_{LT} [eq. (4)].

$$\frac{M}{M_m} = \frac{1 + \zeta\eta v_f}{1 - \eta v_f} \tag{1}$$

$$\eta = \frac{M_r - 1}{M_r + \zeta} \tag{2}$$

$$\zeta = 2\frac{L}{d} \tag{3}$$

$$\upsilon_{LT} = \upsilon_f v_f + \upsilon_m v_m \tag{4}$$

where v_f, v_m = Fiber and matrix volume fraction of composite, M = Composite material modulus E_T, G_{LT} or υ_{LT} (E_T: Transverse Young's modulus, G_{LT}: In-plane shear modulus, υ_{LT}: Longitudinal Poisson's ratio of the unidirectional transversely isotropic short fiber composite), M_r = Ratio of M_f to M_m, M_f = Corresponding fiber modulus E_f, G_f, or υ_f (E_f: Young's modulus of isotropic fibers, G_f: Shear modulus of isotropic fibers), M_m = Corresponding matrix modulus E_m, G_m, or υ_m (E_m: Young's modulus of isotropic matrix, G_m: Shear modulus of isotropic matrix), υ_f, υ_m = Posion's ratio of fiber and matrix, L = fiber length, d = fiber diameter.

ζ is correlated with the geometry of the reinforcement, and it was found empirically for circular fiber in a square array that predictions for E_T are best if $\zeta = 2$, for G_{LT} are best if $\zeta = 1$ and for E_L, ζ can be calculated by eq. (3).[17] The subscriptions L and T denote longitudinal and transverse direction, respectively. M and f represent fiber and matrix.

To enhance the composites performance, improve the system reliability and reduce life/cycle cost, it is essential to have a thorough understanding of the interaction of shape and orientation together on the fracture mechanism in short fiber reinforced composites. This research focuses on the effect of fiber shape and its orientation on the modulus of epoxy-based composite and crack growth behavior. The predicted Young's modulus of the composite is compared with that obtained from experimental results. Finally, the crack growth direction was also observed. The main aim of this work is to bring insight for the application of fibers in composites to provide flexibility in design and mechanical properties.

EXPERIMENTAL PART

Materials

Bisphenol A Epichlorohydrin-based epoxy resin with *n*-butyl glicidyl ether with a cycloaliphatic polyamine catalyst were obtained from Aldrich, Germany. Carbon steel fibers were purchased from China National Building Materials Corporation, China. The diameter of carbon steel fiber was 0.6 mm. Approximately 23% by weight of catalyst was added to the epoxy resin (shown in Table I).

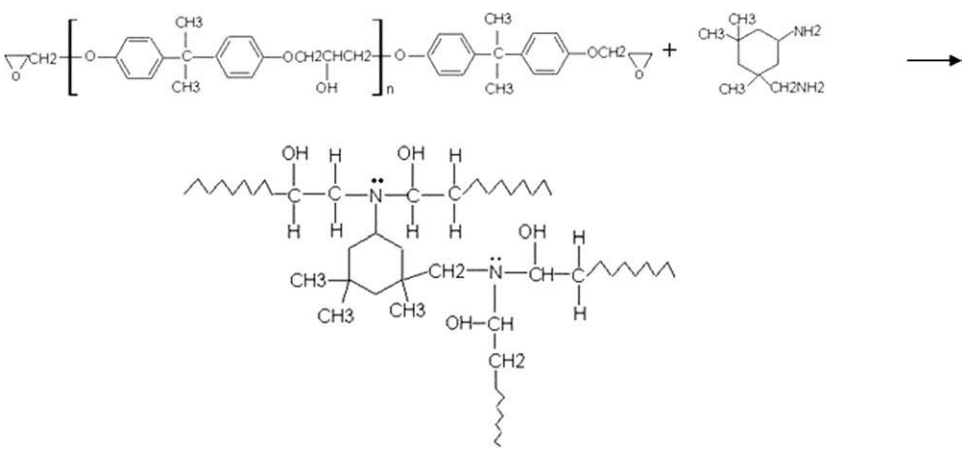

Figure 1 Crosslinking mechanism of Bisphenol A Epichlorohydrin-based epoxy resin with Cycloaliphatic polyamine curing agent.

Figure 2 Different shapes of steel fiber.

Crosslink's mechanism of bisphenol A Epichlorohydrin-based epoxy resin with cycloaliphatic polyamine curing agent is shown in Figure 1.

Preparation method

A minimum of five test samples for strength assessment for each fiber-matrix combination were prepared and tested. Two fiber lengths of 15 and 30 mm were used in the experiments with fiber geometries in the form of straight, waved, and endhooked as shown in Figure 2. Tensile specimens shape is illustrated in Figure 3, corresponding to ASTM D638-02, type I. All of the composites were reinforced with 1.7% volume fraction of fibers. The samples were cured at room temperature for 48 h. Tensile specimens were tested using Zwick tester machine model 1446-60 with 10 KN load cell at a crosshead speed of 5 mm/min.

To remove the air from the Epoxy matrix, centrifuging was used in specimen preparation. Specimens were prepared by pouring half of the required mixed matrix into a silicone rubber mold and after 24 h curing at room temperature; the fibers were added to the mold with an orientation show in Table II.

Residual of the mixed matrix was poured into the mold and allowed to cure for a further 24 h at room temperature. The sample was removed from the mold, and its width and thickness were measured with a micrometer and then was tested.

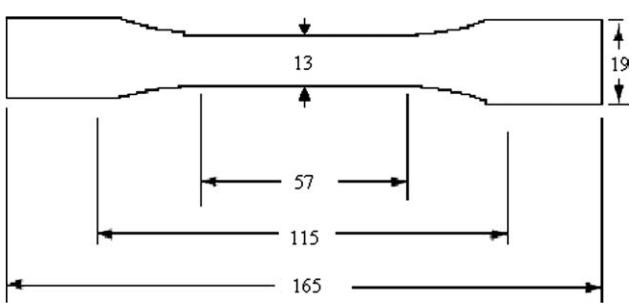

Figure 3 Diagram of the tensile specimen used in this study, corresponding to ASTM D638-02, specimen type I.

TABLE II
Different Fiber Orientations in Sample Composites

Fiber orientation schematic in composite	Angle	Mode
	0°	1
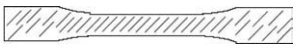	45°	2
	0°/45°	3

RESULTS AND DISCUSSION

Experimental results

Under the same loading conditions, higher stiffness means a greater contribution of the fibers, which suggests more load transfer to the fiber by fiber/matrix interface, corresponding to a better load bearing by fiber. Longitudinal Young's modulus is the most fundamental elastic constant. Young's moduli were determined from the slope of the initial linear part of the stress–strain curves. Table III shows the results of composite's modulus reinforced with waved and straight fiber with 15 mm length and waved and endhooked fiber with 30 mm length. The results show that by decreasing the average angle between fiber alignment and loading direction, the modulus of both waved fiber-reinforced composite and straight fiber-reinforced composite will increase, but the extent of increase is not the same. By changing straight fiber orientation from mode 1 through mode 3, the composite modulus will change in the order of 73%, 16%, and 53%, and for waved fiber, the change is in the order of 45%, 24%, and 44%. Comparison between waved fiber-reinforced and straight fiber-reinforced composite shows that for

TABLE III
Experimental Results for Modulus of Composite Reinforced with Waved, Straight, and Endhooked Fiber

Mode	1 (GPa)	2 (GPa)	3 (GPa)	3* (GPa)
Fiber shape and length				
Waved (15 mm)	2.99	2.55	2.95	2.81
Straight (15 mm)	3.54	2.33	3.15	3.07
Waved (30 mm)	3.40	–	–	–
Endhooked (30 mm)	3.95	–	–	–

*Predicted results for mode 3 using law of mixture with 60% mode 1 and 40% mode 2 using experimental results obtained.

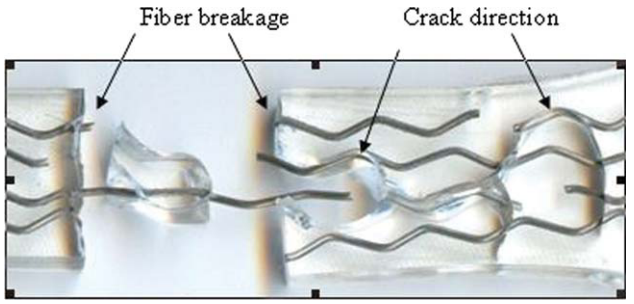

Figure 4 Direction of crack propagation for the composite reinforced with 30 mm waved fiber. [Color figure can be viewed in the online issue, which is available at wileyonlinelibrary.com.]

composite with mode 2 orientation, modulus of straight fiber-reinforced composites is lower than that of waved fiber-reinforced composites. This is explained by Halpin-Tsai prediction section presented later.

The angle in the composite reinforced with waved fiber is between a line that connects the beginning and end of the fiber relative to the loading direction. According to this definition for orientation mode 2, the angle between portions of a fiber, (due to the waved structure) with loading direction is not 45°. Our analysis shows that one portion of the waved fiber has an average angle of 15°, and the other portion has an average angle of 63° relative to the loading direction.

The result obtain for endhooked fiber-reinforced composite (mode 1, length 30 mm) has higher modulus than the waved fiber-reinforced composite this could be due to the following reasons.

1. Suitable mechanical interlocking in the fiber end and matrix as a result of fiber end shape.
2. Greater portion of the fiber axis was parallel to the loading direction.

Direction of crack propagation indicates that it is influenced by the fiber shape as shown in Figure 4. Crack direction has a different angle relative to the loading direction, and therefore, much more energy would be consumed during crack propagation, this will significantly improve toughness.

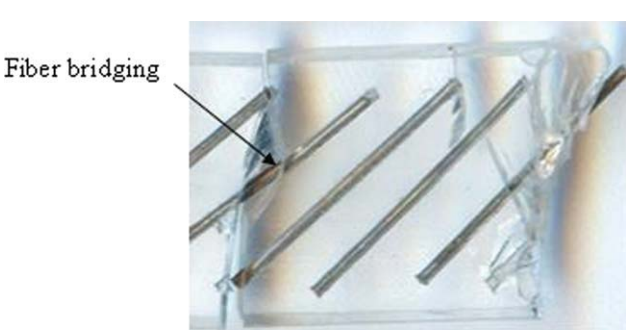

Figure 5 Carbon steel fiber bridging on the crack face. [Color figure can be viewed in the online issue, which is available at wileyonlinelibrary.com.]

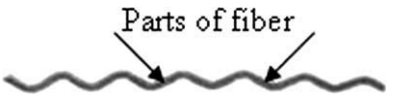

Figure 6 Parts of waved fiber.

It can be noted from Figures 4 and 5 that the lengths of the waved and straight fibers are higher than the critical length. Fiber breakage is shown in Figure 4, and fiber bridging is shown in Figure 5.

Young's modulus prediction using Halpin-Tsai equation

Longitudinal Young's modulus of composite reinforced with straight and waved fiber obtained experimentally is compared with the result obtained using Halpin-Tsai semi-empirical equation. Table I shows material properties of composite's components, which are used for theoretical calculations. The effective Young's modulus of the composite along the loading direction, E_x, can be obtained by replacing E_L, υ_{LT}, E_T, G_{LT}, and υ_{LT} calculated by eqs. (1)–(4) into eq. (5).[18] The step by step calculation of G_{LT} and υ_{LT} as an example is presented in appendix

$$\frac{1}{E_x} = \frac{\cos^4\theta}{E_L} + \frac{\sin^4\theta}{E_T} + \frac{1}{4}\left(\frac{1}{G_{LT}} - \frac{2\upsilon_{LT}}{E_L}\right)\sin^2 2\theta \qquad (5)$$

In calculating E_x for waved fiber composite, the following steps have been taken.

1. Assuming two portions for the fiber as showed in Figure 6.
2. Calculating the average angle made by each portion for mode 2 arrangement, these angles are 15° and 63°.
3. Percentage of fiber's portion for above angles taken as 50% for the fiber arrangement mode 2.

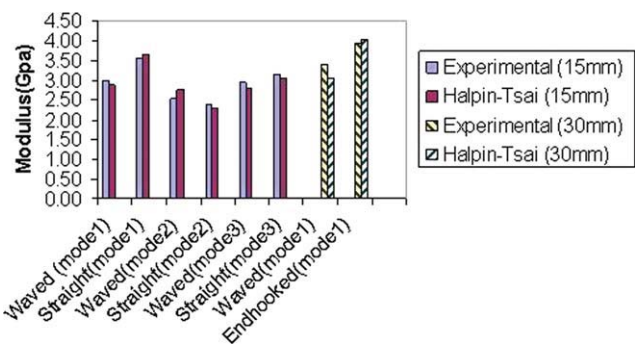

Figure 7 Modulus results obtained from experimental and calculated moduli using Halpin-Tsai equation. [Color figure can be viewed in the online issue, which is available at wileyonlinelibrary.com.]

TABLE IV
Volume Percentage Related to Fiber Angle with Loading Direction for Different Fiber Shapes and Orientation

	1		2		3	
Mode	% v_j	Angle	% v_j	Angle	% v_j	Angle
Fiber shape						
Straight	100	0.0°	100	44.4°	50	0°
	–	–	–	–	50	48.0°
Waved	100	25.0°	50	15.0°	25	22.7°
	–	–	50	63.0°	50	29.5°
	–	–	–	–	25	67.0°
Endhooked	88	0.0°	–	–	–	–
	12	48.0°	–	–	–	–

4. It has been assumed that composite reinforced with waved fiber is equivalent to a composite reinforced with flat fibers having 50% of the fibers aligned with 63° to the loading direction and 50% of the fibers aligned with 15° to the loading direction.
5. For each of the above percentages using eq. (5), E_{x1} and E_{x1} have been calculated.
6. For the assumed composite in step 4, E_x represents its modulus and has been calculated by eq. (6).

$$E_x = \%xE_{x1} + \%yE_{x2} \tag{6}$$

Experimental Young's modulus results and Halpin-Tsai calculated moduli for composite reinforced with waved and straight fibers are shown in Figure 7; the results indicate that there is a good agreement between experimental Young's modulus and Halpin-Tsai calculated moduli for all the composites in this research work. Similar analysis was carried out for composite Model 1, Model 2, and endhooked fibers, and the results are also shown in Figure 7.

The ratio of E_x to E_L is plotted versus fiber angle with loading direction using eq. (7) and Table IV (Fig. 8) for straight and waved fiber composite. Dimensions of the 2217 and 3646.85 in the eq. (7) is MPa, and the dimension of 2.5727×10^{-4} is 1/MPa.

$$\frac{1}{E_x} = \frac{\cos^4\theta}{3646.58} + \frac{\sin^4\theta}{2217} + 2.5727{*}10^{-4}(\sin 2\theta)^2 \tag{7}$$

As it can be noticed from the results presented in Table III for mode 2 orientation and Figure 8, the waved fibers have higher moduli compared to the straight fiber composites; these results can be justified by plotting $dE_x/d\theta$ versus θ as shown in Figure 9. It can be noticed that maximum increase

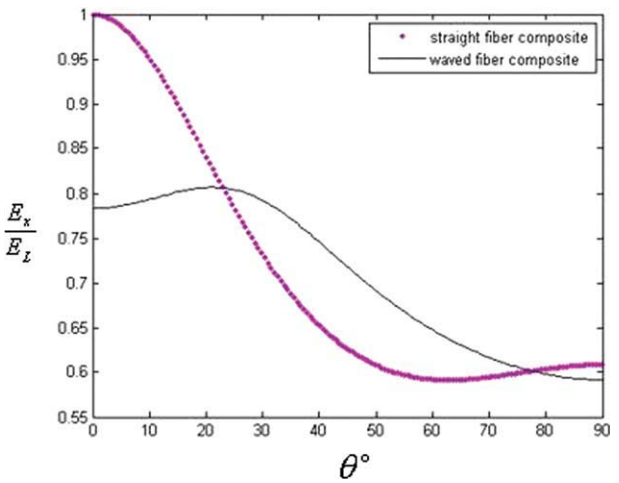

Figure 8 Plot of $\frac{E_x}{E_L}$ versus fiber angle relative to the longitudinal direction for straight and waved fiber composites. [Color figure can be viewed in the online issue, which is available at wileyonlinelibrary.com.]

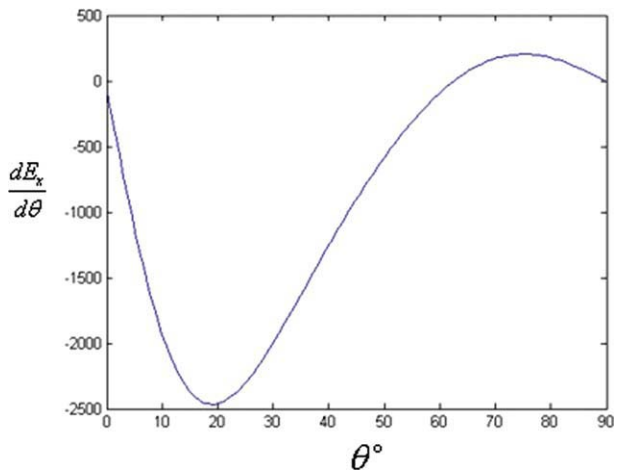

Figure 9 Plot of $\frac{dE_x}{d\theta}$ versus fiber angle relative to the loading direction. [Color figure can be viewed in the online issue, which is available at wileyonlinelibrary.com.]

and decrease of modulus occur at 18° and 74°, respectively. When a waved fiber is used in mode 2 with 45° angle relative to loading direction, the increase of modulus from 15° portion of the waved fibers is higher than the decrease obtained from the 63° portion. Therefore, mode 2 orientation for waved fibers produces higher modulus than the straight fibers.

CONCLUSIONS

From the results obtained, it can be concluded that the shape of waved fibers can influence modulus of composite in a given orientation. Waved fiber can easily be obtained by texturing procedure technology. Crack propagation and bridging of fiber across a crack are also influenced by waved shape. The experimental results obtained are in good agreement with the theoretical predictions calculated by Halpin-Tsai equation. The results presented here can give a very good insight into the application of textured fibers used as reinforcement. This could provide design flexibility and improvement in mechanical properties at different angles.

APPENDIX

Calculations of υ_{LT} and G_{LT} are presented here. Calculations of others input for eq. (5) such as E_L, E_T are the same as calculations of G_{LT}, with only difference is the replaced value of ζ base on the description given in the article.

To calculate υ_{LT}, we used eq. (4) (rule of mixture). Therefore, by placing the fiber and matrix possion's ratio and the fiber and the matrix volume fraction of composite in this equation, we can calculate υ_{LT}.

$$\upsilon_{LT} = \upsilon_f v_f + \upsilon_m v_m$$
$$\upsilon_{LT} = 0.3 * 0.027 + 0.28 * 0.973 = 0.28$$

To calculate $G_{LT,}$ it is needed to calculate G_f and G_m. For calculating the G_f and G_m we used equation $G_f = \frac{E_f}{2(1+\upsilon_{LT})}$ and $G_m = \frac{E_m}{2(1+\upsilon_{LT})}$. Fiber and matrix young's moduli were determined from the slope of the initial linear part of the stress–strain curves of fiber and matrix, respectively.

$$G_f = \frac{135.8}{2(1+0.28)} = 52.25(\text{GPa})$$

$$G_m = \frac{2.05}{2(1+0.28)} = 0.80(\text{GPa})$$

To calculate η, we used eq. (2) $\left(\eta = \frac{M_r - 1}{M_r + \zeta}\right)$. In using this equation with the aim of G_{LT} calculation, M_r is equal to $\frac{G_f}{G_m}$ and so it becomes 65.31. As it is mentioned earlier, prediction for G_{LT} is best if ζ=1. Therefore, we have the following step for the calculation of η.

$$\eta = \frac{65.31 - 1}{65.31 + 1} = 0.97$$

In next step, eq. (1) can be used for the calculation of G_{LT}. As it is mentioned before M means composite material modulus, and therefore, M_m means corresponding matrix modulus. Therefore, in the case of G_{LT} calculation, we can replace M and M_m with G_{LT} and G_m, respectively. Thus, we have the following final step for calculation of $G_{LT.}$

$$G_{LT} = G_m\left(\frac{1+\zeta\eta v_f}{1-\eta v_f}\right) = 802*\left(\frac{1+0.97*0.027}{1-0.97*0.027}\right) = 845(\text{GPa})$$

References

1. Wetherhold, R. C.; Bös, J. Theor App Fract Mech 2000, 33, 83.
2. Fara, S.; Pavan, J. Mater Sci 2004, 39, 3619.
3. Hsueh, C. H. Compos Sci Technol 2000, 60, 2671.
4. Wrtherhold, R. C.; Corjon, M.; Das, P. K. Compos Sci Technol 2007, 67, 2428.
5. Bagwell, R. M.; Wrtherhold, R. C. Compos A 2005, 36, 683.
6. Zadhoush, A.; Sheikhzadeh, M.; Elahidust, A.; Pirzadeh, E. Polym Compos 2010, 31, 203.
7. Zhu, Y. T.; Valdez, J. A.; Beyerlein, I. J.; Zhou, S. J.; Liu, C.; Stout, M. G.; Butt, D. P.; Lowe, T. C. Acta Mater 1999, 47, 1767.
8. Zhu, Y. T.; Beyerlein, I. J Mater Sci Eng A 2002, 326, 208.
9. Zhou. Y. Ph.D. Theses, University of Notre Dame, Aerospace and Mechanical Engineering department, 2005.
10. Bagwell, R. M.; Wrtherhold, R. C. Mater Sci Eng A 2003, 361, 294.
11. Wrtherhold, R. C.; Das, P. K. Mater Sci Eng A 2007, 460–461, 344.
12. Tsai, J.; Patra, A. K.; Wrtherhold, R. C. Compos A 2003, 34, 1255.
13. Bagwell, R. M.; Wrtherhold, R. C. Theor Appl Fract Mec 2005, 43, 181.
14. Wrtherhold, R. C.; Lee, F. K. Compos Sci Technol 2001, 61, 517.
15. Bagwell, R. M.; Wrtherhold, R. C. J Adhes Sci Technol 2003, 17, 2223.
16. Bagwell, R. M.; Mcmanaman, M. J.; Wrtherhold, R. C. Compos Sci Technol 2006, 66, 522.
17. Jones, R. M. Ph.D. Theses, Swiss federal institute of technology Zurich, Switerland, 1973.
18. Hall, D. In An Introduction to Composite Material; Chan, R. W., Thompson, M. W., Ward, I. M., Eds.; Cambridge University: Cambridge, 1981; Chapter 6.